ARTHRITIS & RHEUMATISM
Vol. 62, No. 10, October 2010, pp 2995–3005
DOI 10.1002/art.27608

Alteration of Sensory Neurons and Spinal Response to an Experimental Osteoarthritis Pain Model

Hee-Jeong Im,[1] Jae-Sung Kim,[2] Xin Li,[2] Naomi Kotwal,[2] Dale R. Sumner,[2] Andre J. van Wijnen,[3] Francesca J. Davis,[2] Dongyao Yan,[2] Brett Levine,[2] James L. Henry,[4] Jacques Desevré,[5] and Jeffrey S. Kroin[2]

Objective. **To verify the biologic links between progressive cellular and structural alterations within knee joint components and development of symptomatic chronic pain that are characteristic of osteoarthritis (OA), and to investigate the molecular basis of alterations in nociceptive pathways caused by OA-induced pain.**

Methods. **An animal model of knee joint OA pain was generated by intraarticular injection of monoiodoacetate (MIA) in Sprague-Dawley rats, and symptomatic pain behavior tests were performed. Relationships between development of OA with accompanying pain responses and gradual alterations in cellular and structural knee joint components (i.e., cartilage, synovium, meniscus, subchondral bone) were examined by histologic and immunohistologic analysis, microscopic examination, and microfocal computed tomography. Progressive changes in the dynamic interrelationships between peripheral knee joint tissue and central components of nociceptive pathways caused by OA-induced pain were examined by investigating cytokine production and expression in sensory neurons of the dorsal root ganglion and spinal cord.**

Results. **We observed that structural changes in components of the peripheral knee joint correlate with alterations in the central compartments (dorsal root ganglia and the spinal cord) and symptomatic pain assessed by behavioral hyperalgesia. Our comparative gene expression studies revealed that the pain pathways in MIA-induced knee OA may overlap, at least in part, with neuropathic pain mechanisms. Similar results were also observed upon destabilization of the knee joint in the anterior cruciate ligament transection and destabilization of the medial meniscus models of OA.**

Conclusion. **Our results indicate that MIA-induced joint degeneration in rats generates an animal model that is suitable for mechanistic and pharmacologic studies on nociceptive pain pathways caused by OA, and provide key in vivo evidence that OA pain is caused by central sensitization through communication between peripheral OA nociceptors and the central sensory system. Furthermore, our data suggest a mechanistic overlap between OA-induced pain and neuropathic pain.**

Chronic pain is a prominent symptom of osteoarthritis (OA), but few studies have examined its role in the etiology of the disease (1). OA is already a major public health problem, and aging of the US population will substantially increase the occurrence of OA-related disability over the next decade. It remains to be established what causes pain in OA, and there is currently no effective treatment to relieve the pain induced by OA.

Nociceptors are located throughout the joint in the capsule, ligaments, menisci, periosteum, and subchondral bone (2). Data from previous studies on OA pain suggest that cellular and structural changes within the peripheral joint components may be the sources of

Supported by grants to Dr. Im from the NIH (National Institute of Arthritis and Musculoskeletal and Skin Diseases grant R01-AR-053220), the Arthritis Foundation, and the National Arthritis Research Foundation.

[1]Hee-Jeong Im, PhD: Rush University Medical Center and University of Illinois at Chicago; [2]Jae-Sung Kim, PhD, Xin Li, MD, PhD, Naomi Kotwal, BE, Dale R. Sumner, PhD, Francesca J. Davis, PhD, Dongyao Yan, BS, Brett Levine, MD, MS, Jeffrey S. Kroin, PhD: Rush University Medical Center, Chicago, Illinois; [3]Andre J. van Wijnen, PhD: University of Massachusetts Medical School, Worcester; [4]James L. Henry, PhD: McMaster University, Hamilton, Ontario, Canada; [5]Jacques Desevré, MS: Bioseb, Vitrolles, France.

Drs. Im and Kim contributed equally to this work.

Address correspondence and reprint requests to Hee-Jeong Im, PhD, Rush University Medical Center, Cohn Research Building, Suite 516, 1735 West Harrison, Chicago, IL 60612. E-mail: Hee-Jeong_Sampen@rush.edu.

Submitted for publication October 30, 2009; accepted in revised form June 8, 2010.

heightened nociception within the arthritic joint (3). Mechanical stimulation of peripheral knee joint components promotes biochemical sensitization and may activate nociceptors located on the afferent nerve fibers of either primary lesions in the cartilage (4–6) or subchondral bone (7). Nevertheless, understanding of the cause of pain in knee OA remains elusive because cartilage, which is the primary site of pathology in OA, lacks pain fibers (8).

Our prior studies demonstrated high expression of multiple inflammatory cytokines, as well as neuropeptides, in synovial fluid, synovium, joint capsular tissue, and cartilage from OA patients with severe pain (9). These inflammatory cytokines may further increase the biologic function of pain mediators by stimulating their cognate receptors, contributing to clinically symptomatic pain perception (10–12). Investigation of OA-related pain mechanisms may lead to elucidation of how peripheral tissue injury transmits pain-provoking signals caused by OA and alters nociceptive pathways.

Several animal models of OA, including spontaneous, surgically induced, or nonsurgically induced OA models, have provided biologic insights into OA-induced progressive pathologic changes in knee joint structures (13) and OA-associated pain behavior (14). Comparative gene array data demonstrate substantial differences between the mono-iodoacetate (MIA)–induced OA animal model and human OA (15). Nevertheless, many other investigators have shown that intraarticular injection of MIA, which is an inhibitor of glycolysis that disrupts metabolism in chondrocytes, causes joint tissue damage that may mimic clinical OA in patients (16–25).

In this study, we verified the utility of the MIA-induced OA animal model to pursue our investigation of the nociceptive pathways caused by OA. We determined the correlations between progressive cellular and structural alterations within the knee joint components and symptomatic chronic pain development, by performing behavior tests in this animal model using a range of different concentrations of MIA over time (0.125–2 mg per knee joint over 5 weeks). Using this verified animal model, we examined whether defective peripheral OA-affected regions can alter central components of nociceptive pathways in the dorsal root ganglia (DRGs) and the dorsal horn of the spinal cord. Our results suggest that activation of peripheral nociceptors is centrally sensitized, stimulating inflammatory cytokines at the level of sensory neurons and spinal cord. Furthermore, the findings indicate that pain caused by MIA-induced OA exhibits sensorineuronal responses that are similar to those observed in neuropathic pain models, suggesting mechanistic overlap in these 2 pain pathways.

MATERIALS AND METHODS

Induction of OA. The procedures used in this study were in compliance with the guidelines of the Rush Institutional Animal Care and Use Committee. Sprague-Dawley rats (weight 200–220 gm) were housed under standard laboratory conditions (in a temperature-controlled room [21°C [±1°C] with a normal 12-hour light/dark cycle). Animals retained full mobility and continued to grow normally. For induction of arthritis with MIA, rats were anesthetized with isoflurane (Abbott) in oxygen and administered a single percutaneous intraarticular injection of 0.125, 0.25, 0.5, or 2.0 mg of MIA (catalog no. I2512; Sigma) or saline vehicle through the infrapatellar ligament of the left knee (n = 8 in each dose group). MIA was dissolved in physiologic saline and administered in a volume of 25 μl using a 26-gauge 0.5-inch needle. The right contralateral knee was used as a behavioral and histologic control. Anterior cruciate ligament transection (ACLT) and destabilization of the medial meniscus surgical instability models of OA were induced as previously described (26).

Animal behavior tests. *Thermal hyperalgesia.* Responses to noxious thermal stimuli were determined using a thermal plantar device according to the procedure described by Hargreaves et al (27), before and at defined times during the 31-day period post–MIA injection. Rats were placed in opaque plastic chambers (22 cm in width × 17 cm in length × 14 cm in height) above a glass plate, for 10 minutes prior to the start of each experiment. The animals were allowed to adjust to their new environment before testing. A movable infrared radiant heat source was placed directly under the glass plate aimed at the plantar surface of the hind paw, and the time taken for hind paw withdrawal was monitored. A cutoff time of 20 seconds was used to avoid tissue damage. Two tests were carried out at 10-minute intervals, and the mean value was taken as the nociceptive threshold.

Mechanical allodynia. Testing for mechanical allodynia was performed according to the method described by Chaplan et al (28). After rats were allowed to acclimate for 15 minutes on a wire mesh grid, a calibrated set of von Frey filaments (Stoelting) was applied from below to the plantar hind paw to determine the 50% force withdrawal threshold using an iterative method. The filament forces ranged from 0.04 to 15 gm, beginning with 2.0 gm. The filament was applied to the skin with enough pressure to buckle, and was maintained for up to 6 seconds. A brisk lifting of the foot was recorded as a positive response. If no response was observed, the filament with the next highest force was applied, while the filament with the next lowest force was applied upon a positive response.

A knee extension test was performed on both legs, starting with the knee in resting position (slightly flexed). While the thigh was held, the knee was extended. The number of vocalizations in 5 extensions was counted. A knee squeeze test was performed on both legs by holding the knee between the thumb and forefinger in a medial–lateral direction. The knee was squeezed firmly (but not so strongly that the unin-

jected leg responded), and the number of vocalizations in 5 squeezes was counted.

Knee edema. The cross-sectional area of the injected knee and the contralateral control knee were measured with calipers to determine the time course of edema.

Computerized incapacitance meter system. The DWB (dynamic weight bearing; Bioseb) is a computerized incapacitance meter system in which behavioral observations are made with the animals on 4 paws in free ambulation, which is consistent with the use of quadrupeds; thus, there is no observation bias. Study of dynamic weight bearing is an important aspect of basic and preclinical research due to the weight redistribution on other body parts (i.e., the front limbs). Decreased paw surface was quantified as OA-induced impairments in paw positioning. During the data capture, the raw data on each paw were synchronized with the images from a video camera and the averaged values were encrypted and recorded on a computer with a sampling rate of 10 Hz, providing accurate and nonbiased pain assessment. The weight distribution of the animal, per limb, with the mean and the coefficient of variation, was then shown in the result window, for each time period.

Tissue preparation. Human articular synovial tissue from knees was obtained from tissue donors through the Gift of Hope Organ and Tissue Donor Network (normal tissue specimens) and Rush Orthopedic Depository Studies (surgically removed OA tissue). For normal tissue, each donor specimen was graded for gross degenerative changes based on a modified version of the 5-point scale of Collins (29). At 2 weeks and 5 weeks after MIA or saline injection, the animals were killed with halothane anesthesia. The entire knee joints were then dissected for histologic, immunohistochemistry, and microscopic analyses and microfocal computed tomography (micro-CT) imaging evaluation. Bilateral lumbar DRGs and dorsal horns of the spinal cords were harvested under light microscopy for further analyses.

Histologic analysis. When the animals were killed, each knee was dissected aseptically, fixed in 4% paraformalin, and then decalcified in EDTA, which was changed every 5 days. The decalcified knee was cut in the midsagittal plane, and paraffin embedded. Serial knee sections of exact 5 μm thickness from the middle part of the knee were obtained to prepare slides. Safranin O–fast green staining was performed to assess general morphology and the loss of proteoglycan in cartilage ground substance. Human synovium and rat knee joints were stained with hematoxylin and eosin to assess general morphology and neovascularization. For immunohistochemistry analysis of neurofilament, medium-chain rabbit polyclonal antibody (catalog no. PA1-84587; Thermo Scientific), which specifically recognizes both human and rat proteins, was used in a 1:500 dilution. All samples from both knees were stained, and samples were examined independently by 2 observers (H-JI and XL).

Microscopic analyses and micro-CT. Structural alterations of articular cartilage surface and subchondral bone architecture were evaluated by microscopic examination and micro-CT scanning. Freshly dissected tibias and femurs were immediately fixed in 10% formalin, followed by micro-CT imaging analyses performed at the Rush Imaging Core Facility, using a Scanco Model 40 Desktop micro-CT. Microscopic analyses were performed to examine structural alterations in anterior and inferior articular cartilage, using a Nikon SMZ1000 (model no. 3.2.0). Subchondral bone was assessed in animal groups with and without OA-induced knee pain. Two different concentrations of MIA (0.5 mg and 2.0 mg per leg) and 2 time courses (2 weeks and 5 weeks) were assessed.

Cytokine antibody array and quantification. Entire spinal cords were ejected, and the dorsal horn was dissected under light microscopy. Tissues were lysed by homogenization in radioimmunoprecipitation assay buffer (150 m*M* NaCl, 1% Nonidet P40, 0.5% deoxycholate, 0.1% sodium dodecyl sulfate, and 50 m*M* Tris [pH 7.5]) with protease cocktail inhibitors (Sigma). The total protein concentrations of cell lysates were determined by a bicinchoninic acid protein assay (Pierce). An array for cytokine proteins (Cytokine Array; RayBio) was used to determine relative alterations in the levels of cytokines. Membranes with immobilized antibodies were incubated for 14 hours with 500 μg of total protein from either the control tissue or experimental tissue (degenerated) followed by biotin-conjugated antibodies, then further incubated with horseradish peroxidase–conjugated streptavidin. Immunoreactivity was visualized using the ECL system (Amersham Biosciences) and the Signal Visual Enhancer system (Pierce), which magnifies the intensity of the signal. Densitometric measurement was performed by calculating the integrated density values for each spot (area relative intensity) using a Molecular Imager Versa-doc MP 4000 system and Quantity One-4.5.0 Basic 1-D Analysis software (both from Bio-Rad). The positive control signals on each membrane were used for normalization of signal intensity.

Total RNA isolation and reverse transcription (RT) and real-time polymerase chain reaction (PCR). Lumbar DRGs and spinal dorsal horns were disrupted and homogenized. Total RNA was isolated using TRIzol reagent according to the instructions provided by the manufacturer (Invitrogen). RT was carried out with 1 μg total RNA, using a ThermoScript RT-PCR system (Invitrogen) for first-strand complementary DNA (cDNA) synthesis. For real-time PCR, cDNA was amplified using an MyiQ Real-Time PCR Detection System (Bio-Rad); β-actin was used as an internal control. Deviations in samples represent 3 different donors in 3 separate experiments. Primers used were as follows: calcitonin gene-related peptide (CGRP; NCBI reference no. NM_001033956.1) forward 5′-TCTAGTGTCACTGC-CCAGAAGAGA-3′, reverse 5′-GGCACAAAGTTGTCCTTCACCACA-3′; neuropeptide Y (NCBI reference no. M15793.1) forward 5′-AGATCCAG-CCCTGAGACACT-GATT-3′, reverse 5′-TGGAAGGGTC-TTCAAGCCTTGTTC-3′; galanin (NCBI reference no. NM_033237.1) forward 5′-TCTGTGCCTCAGCCTCTTCTC-ATT-3′, reverse 5′-TTGGGAACTTCTCCTCCTTGTTGG-3′; tumor necrosis factor α (TNFα; NCBI reference no. NM_012675.3) forward 5′-TTCCCACCACTGCTCA-AGATG-3′, reverse 5′-TGGCTGACAGGGTTGCAA-3′; interleukin-1 (IL-1; NCBI reference no. NM_031512.2) forward 5′-TCATCTTTGAAGAAGAGCCCGTCC-3′, reverse 5′-TGCAGTGCAGCTGTCTAATGGGAA-3′; substance P (NCBI reference no. NM_012666.2) forward 5′-TGGTCAGATCTCTCACAAAGG-3′, reverse 5′-TGCATT-GCGCTTCTTTCA-TA-3′; β-actin (NCBI reference no. NM_031144) forward 5′-TGTCACCAAC-TGGGACGATA-TGGA-3′, reverse 5′-AGCACAGGGTGCTCCTCA-3′.

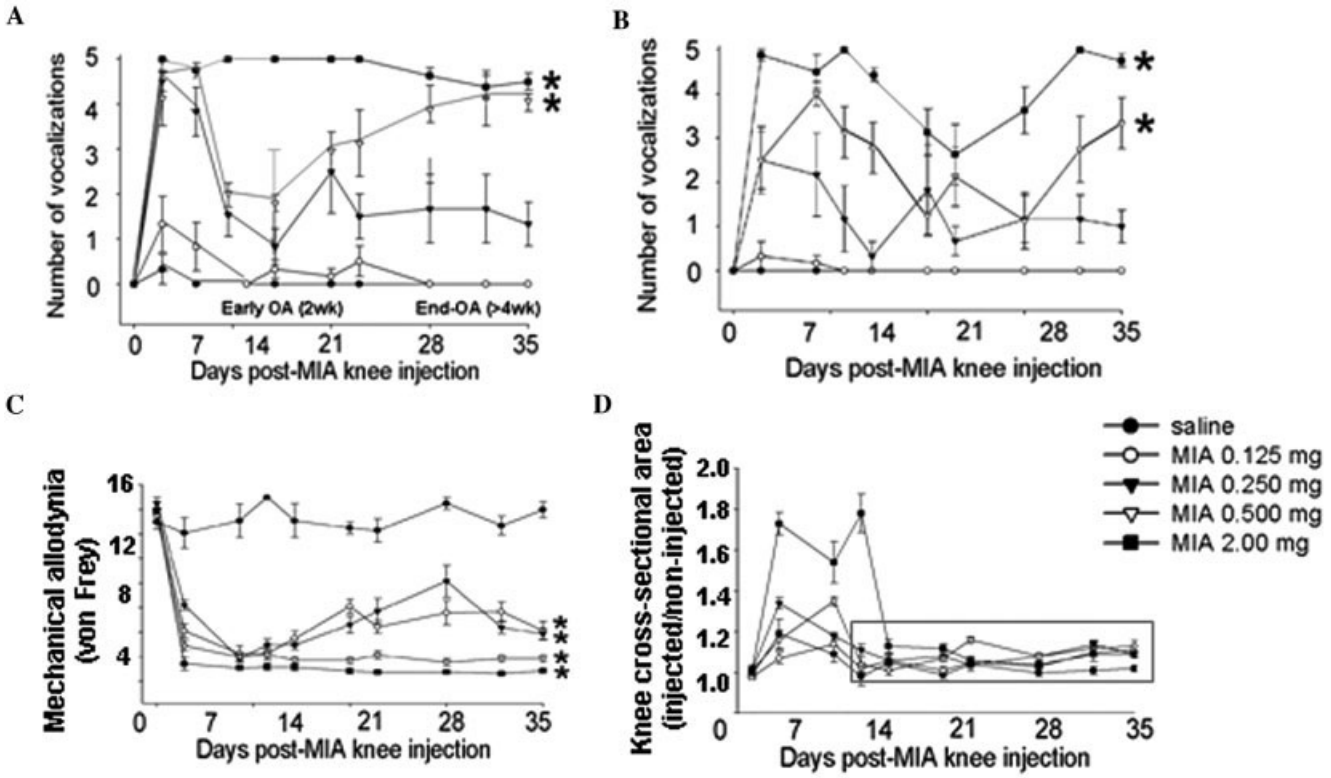

Figure 1. Pain behavior assessments in the mono-iodoacetate (MIA)–induced osteoarthritis (OA) model. A rat model of joint pain was generated by intraarticular injection of MIA (0.125–2 mg) or saline as sham control, and sequential pain behavior tests were performed. **A,** Knee pressure hyperalgesia, assessed by number of vocalizations in response to pressure. **B,** Knee extension hyperalgesia, assessed by number of vocalizations in response to extension. **C,** Mechanical allodynia (von Frey), assessed by 50% force withdrawal threshold, in gm. **D,** Edema in injected knee, assessed by the ratio of the area in injected versus uninjected knees. Representative results from 1 of 2 separate experiments are shown; values are the mean ± SEM (n = 8 rats per treatment group). $* = P < 0.05$ versus saline-treated controls.

Statistical analysis. Results are expressed as the mean ± SEM. Results of repetitive testing of paw withdrawal were analyzed using a repeated-measures general linear model with Student-Newman-Keuls post hoc test. Real-time PCR data were evaluated by one-way analysis of variance with Tukey's post hoc test, using $2^{-\Delta\Delta Ct}$ values for each sample. P values less than 0.05 were considered significant.

RESULTS

Articular injection of MIA increases knee joint discomfort in rats in a dose-dependent manner. A rat model of knee joint pain was generated by intraarticular injection of MIA, after which behavior tests were administered. Sequential pain behavior tests revealed that animals injected with MIA in concentrations of 0.5 mg or 2.0 mg per knee (ipsilateral) exhibited significant increases in joint discomfort in response. The response occurred in a concentration-dependent manner, as determined by increased vocalization in response to knee squeeze ($P < 0.001$) and to knee extension ($P < 0.001$) compared with the contralateral knee and compared with responses to lower concentrations of MIA (0.125 mg or 0.25 mg/joint; n = 8 rats per group) (Figures 1A and B). Interestingly, rats injected with MIA at 0.5 mg/knee joint exhibited time-dependent knee pain behavior, with an early OA phase (2–3 weeks) and an end-stage OA phase (>4 weeks) after the initial period of inflammation (days 7–10) (Figure 1A). Dose-dependent decreases in latency of response to heat (thermal hyperalgesia) (data not shown) and increases in mechanical allodynia (von Frey) (Figure 1C) were also consistently observed 35 days postinjection, when compared with the contralateral side (both $P < 0.001$).

This symptomatic joint discomfort was sustained during the entire joint pain assessment period (>8 weeks) (data not shown), suggesting the development of chronic pain. No significant edema in the injected knee

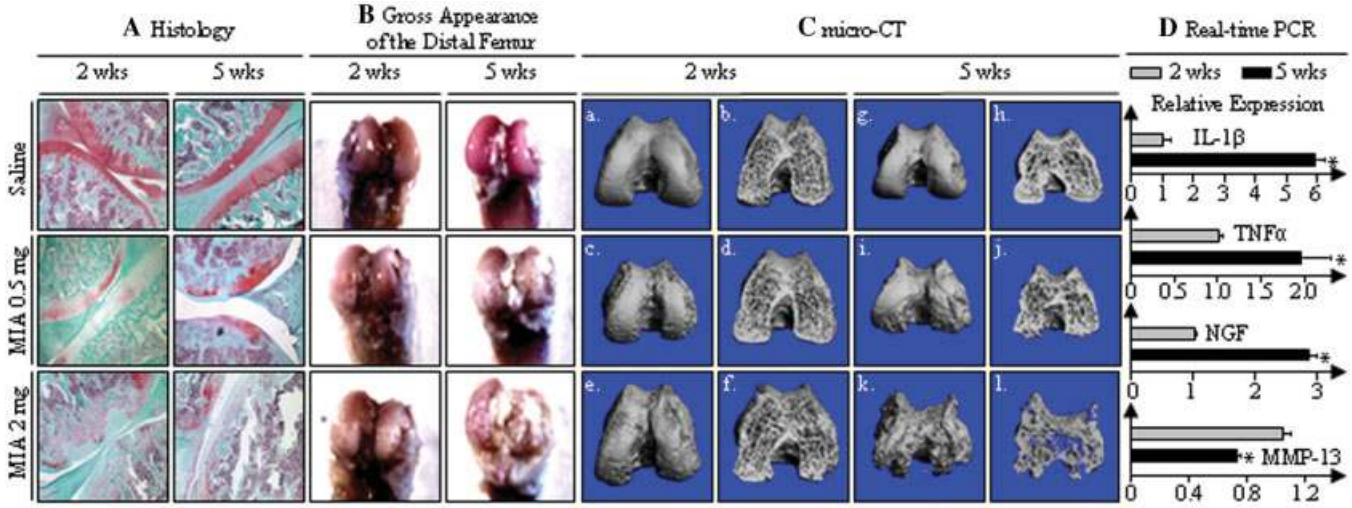

Figure 2. Histologic and morphologic findings and gene expression in the MIA-induced rat OA model. Rats were administered a single intraarticular injection of MIA (0.5 mg or 2 mg per knee) or saline (sham) and were killed 2 weeks or 5 weeks after injection. **A,** Histologic assessment for proteoglycan depletion, determined by Safranin O staining (original magnification × 40). **B,** Microscopic analysis of the gross appearance of the distal femur articular cartilage surfaces. **C,** Architectural changes in subchondral bone structures analyzed by microfocal computed tomography (micro-CT). Views of the distal aspect of the subchondral bone plate of femoral condyles from rats killed 2 weeks (**a**, **c**, and **e**) or 5 weeks (**g,i** and **k**) after intraarticular MIA injection, and distal views of the femoral condyles with the subchondral plate removed to reveal the trabecular bone from rats killed 2 weeks (**b**, **d**, and **f**) or 5 weeks (**h**, **j**, and **l**) after MIA injection are shown. Knees shown in **A–C** are representative of the respective treatment groups (n = 8 per group). **D,** Real-time polymerase chain reaction (PCR) analysis of gene expression levels in cartilage 2 weeks and 5 weeks post–MIA injection. Expression levels are in relation to levels of β-actin. Values are the mean and SEM. $* = P < 0.05$ versus 2-week value. IL-1β = interleukin-1β; TNFα = tumor necrosis factor α; NGF = nerve growth factor; MMP-13 = matrix metalloproteinase 13 (see Figure 1 for other definitions).

was observed after 7–10 days (Figure 1D), indicating that MIA-induced knee joint pain is OA-like chronic pain, and inflammatory responses are not a major component to the sustained pain.

Results of these pain behavior assessments were further verified by measurement of dynamic weight bearing using a computerized incapacitance meter system, in which behavioral observations are made while the animals have free quadrupedal ambulation. These measurements assess consistent use of all 4 paws and whether there was observational bias in other evaluations due to weight redistribution to other body parts (i.e., the front limbs). Our results revealed significant differences ($P < 0.03$) in weight distribution during rearing on hind limbs, between the ipsilateral knees injected with 0.5 mg MIA and the contralateral knees, at 5 weeks post–MIA administration (data not shown).

MIA-induced joint pain correlates with alterations in the structural components of the knee joints and subchondral bone and in chondrocyte gene expression. To evaluate the interrelationship between the symptomatic pain and joint pathology in the MIA-induced knee joint pain model, alterations in structural components of knee joint tissue were examined histologically. We observed time- (2 weeks and 5 weeks) and dose-dependent loss of proteoglycan in the MIA-injected knee joint cartilage and meniscus, by Safranin O staining (Figure 2A). These histologic changes correlated with time- and dose-dependent alterations in the gross appearance of both the anterior and the inferior articular cartilage surfaces (Figure 2B).

Similarly, 3-dimensional micro-CT scanning (Figure 2C) demonstrated structural alterations in the subchondral bone of rats with MIA-induced knee OA, as seen in human OA. Surface rendering of the subchondral plate indicated that the surface topography of MIA-injected joints was considerably altered, in a time- and dose-dependent manner. Administration of 2 mg MIA per knee resulted in a severely heaved and sunken surface at week 5 (Figure 2C, parts k and l) compared with results obtained with a lower dose of MIA (0.5 mg) and assessment at an earlier time point (week 2) (Figure 2C, parts c and d). Saline-injected control knees were not altered, and the joints maintained structural integrity (Figure 2B and Figure 2C, parts a, b, g, and h). In the coronal and sagittal planes of the ipsilateral joints,

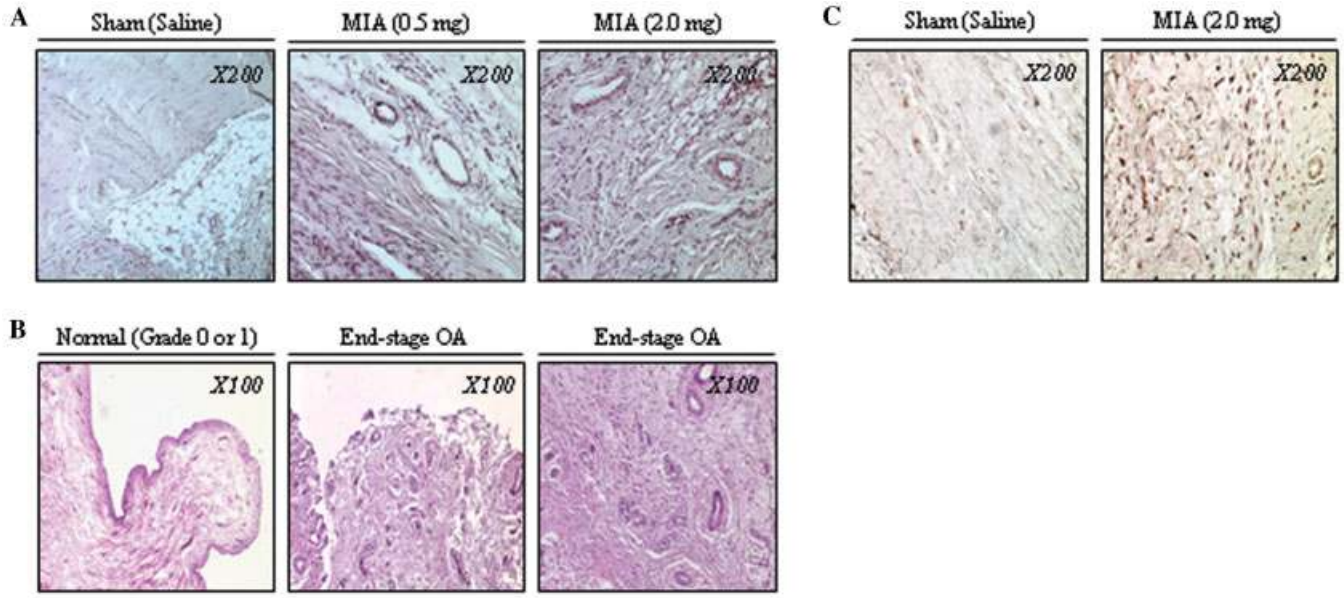

Figure 3. Histologic and immunohistologic assessment of synovium in the MIA-induced rat OA model compared with human OA synovium. Rats were administered a single intraarticular injection of MIA (0.5 mg or 2 mg per knee) or saline (sham) and were killed 5 weeks after injection. **A** and **C,** Structural changes in rat knee joint synovium were assessed by hematoxylin and eosin (H&E) staining, showing increased neovascularization in the synovium of MIA-treated rats (**A**), and nerve ingrowth was assessed based on immunoreactivity of anti–neurofilament M antibody, showing increased ingrowth in the synovium of MIA-treated rats (**C**). **B,** Synovium from normal human subjects and from patients with late-stage OA and knee pain was assessed by H&E staining, showing angiogenesis in the human knee OA synovium. See Figure 1 for other definitions.

pathologic changes were evident in large regions beneath the subchondral plates, reflected by formation of cysts and osteophytes, and structural changes in bone shapes, especially in knee joints injected with 2 mg MIA (Figure 2C, parts k and l).

Collectively, these results suggest that MIA-induced joint pain is correlated with structural alterations in knee joint components and subchondral bone that resemble pathologic alterations characteristic of human OA.

In order to examine the changes in early OA (2 weeks) and end-stage OA (>4 weeks), we further analyzed alterations in gene expression at the early and late stages of disease. Real-time PCR results demonstrated that gene expression patterns in the MIA-induced OA cartilage at 2 weeks and 5 weeks (Figure 2D) were similar to those reported previously (30).

MIA-induced knee OA is associated with angiogenesis in the peripheral knee joint tissue and mimics pathologic changes in human end-stage OA. Synovial angiogenesis may be stimulated during the inflammatory response that accompanies the pathologic progression of OA (31). We examined whether synovium from knees with MIA-induced OA exhibits neovascularization, as is frequently seen in the synovium of OA patients with knee pain. Interestingly, at week 5 there was clear evidence of neovascularization in synovial tissue in hematoxylin and eosin–stained sections from MIA-injected knee joints (Figure 3A). This angiogenic feature in an animal model of OA mimics changes in human synovium from patients with symptomatic OA (Figure 3B). Angiogenesis promotes ingrowth of new sensory nerves into peripheral knee joint tissue exposed to damage and inflammation and can contribute to persistent pain, even after inflammation has subsided (32). Indeed, in our OA model, we observed a significant increase in sensory innervation as reflected by increased neurofilament M immunoreactivity in MIA-injected synovium, compared with synovium from saline-injected and/or contralateral knee joints (Figure 3C).

Alterations in DRG sensory neurons in the MIA-induced OA pain model compared with a neuropathic pain model. To understand the nociceptive pathways that mediate knee joint pain, we investigated peripheral sensory neuronal responses in the MIA-induced knee OA model. The expression levels of cytokines and pain mediators in the L3–L5 DRGs were investigated using real-time PCR. In an analysis of levels of representative inflammation- or pain-related genes in each bilateral lumbar section of DRGs (L1–L6), i.e., L1–L2 (L1),

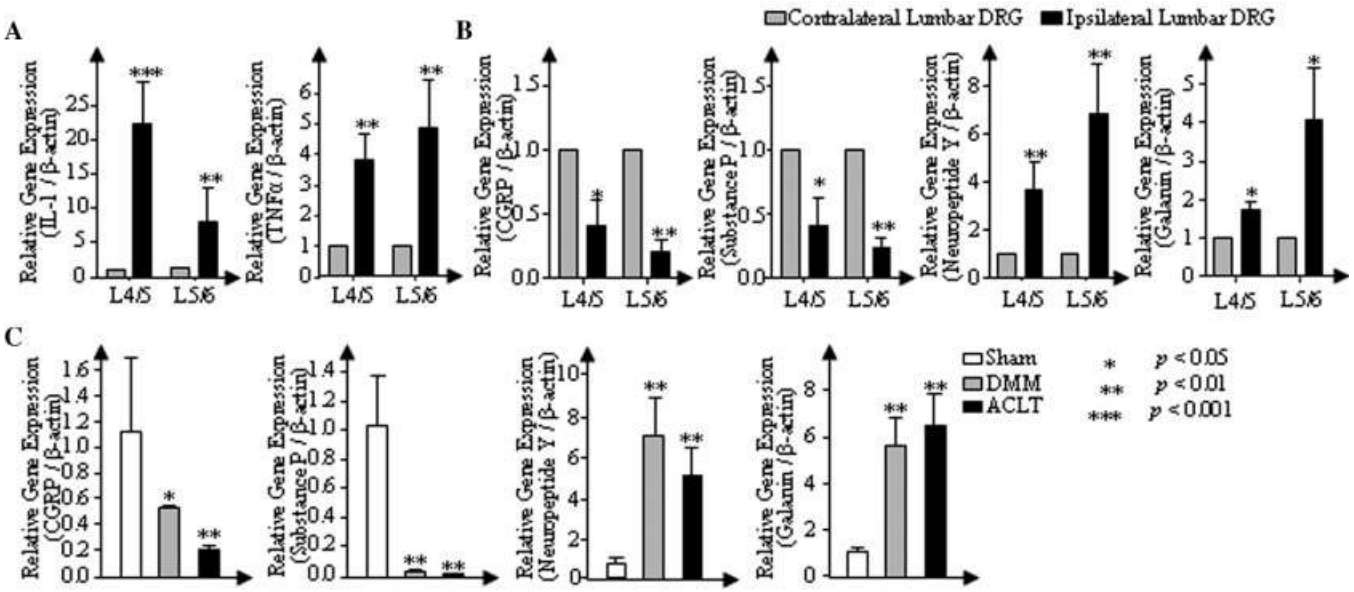

Figure 4. Gene expression analysis in dorsal root ganglia (DRGs) in the mono-iodoacetate (MIA)–induced rat osteoarthritis (OA) model and in other OA models. Rats were administered a single intraarticular injection of MIA (2 mg per knee) or saline (sham) and were killed 5 weeks after injection. Bilateral lumbar DRGs at the levels of L3–L4, L4–L5, and L5–L6 were harvested, and relative expression of target gene mRNA was analyzed by real-time polymerase chain reaction. **A,** Analysis of proinflammatory cytokines (interleukin-1 [IL-1] and tumor necrosis factor α [TNFα]). **B,** Analysis of pain mediators and neuropeptides (calcitonin gene-related peptide [CGRP], substance P, neuropeptide Y, and galanin). **C,** Comparison analyses of gene expression patterns in DRGs (L4–L5) from animals with OA induced using established models (anterior cruciate ligament transection [ACLT] and surgical destabilization of the medial meniscus [DMM]). Values are the mean and SEM. *P* values are versus the contralateral knee (**A** and **B**) or versus sham treatment (**C**).

L2–L3 (L2), L3–L4 (L3), L4–L5 (L4), L5–L6 (L5), and L6–S1 (S1), there were no significant differences (data not shown). Therefore, subsequent analyses were focused on L3–L5 DRGs and examined selected inflammatory cytokines, i.e., IL-1β and TNFα (Figure 4A) or pain mediators and neuropeptides, i.e., CGRP, substance P, neuropeptide Y, and galanin (Figure 4B). These pain-associated genes are significantly up- or down-regulated in other pain pathways, such as neuropathic and inflammatory pain (33). Alterations in sensory neurons in DRGs from animals with MIA-induced knee OA pain were compared with neuronal changes in animals with neuropathic pain. Interestingly, the results showed that gene expression patterns in the 2 pain pathways are strikingly similar, suggesting that pain provoked by OA may be mediated in part through neuropathic pain mechanisms.

To ensure that the rat model of MIA-induced knee pain is appropriate for translational OA pain studies, we also compared gene expression patterns in DRGs using 2 alternative established animal models of OA, i.e., destabilization surgery by ACLT and destabilization of the medial meniscus (Figure 4C). As summarized in Table 1, our data suggested that all 3 rat models of OA-induced pain (i.e., ACLT, medial meniscus destabilization, and intraarticular injection of MIA) exhibit similar gene expression patterns in DRGs. Taken to-

Table 1. Altered gene expression in the sensory neurons in DRGs in a neuropathic animal model compared with rat models of OA knee joint pain*

Gene	Neuropathic model (SNL)	OA knee pain models		
		MIA-induced	ACLT	DMM
DREAM	↑	↑	↑	↑
TNFα	↑	↑	↑	↑
CGRP	↓	↓	↓	↓
Substance P	↓	↓	↓	↓
Galanin	↑	↑	↑	↑
Neuropeptide Y	↑	↑	↑	↑
IL-1α/β	↑	↑	↑	↑

* Patterns of up-regulation or down-regulation relative to sham control are indicated by arrows. DRGs = dorsal root ganglia; OA = osteoarthritis; SNL = spinal nerve ligation; MIA = mono-iodoacetate; ACLT = anterior cruciate ligament transection; DMM = surgical destabilization of the medial meniscus; DREAM = DRE antagonist modulator; TNFα = tumor necrosis factor α; CGRP = calcitonin gene-related peptide; IL-1α/β = interleukiin-1α/β.

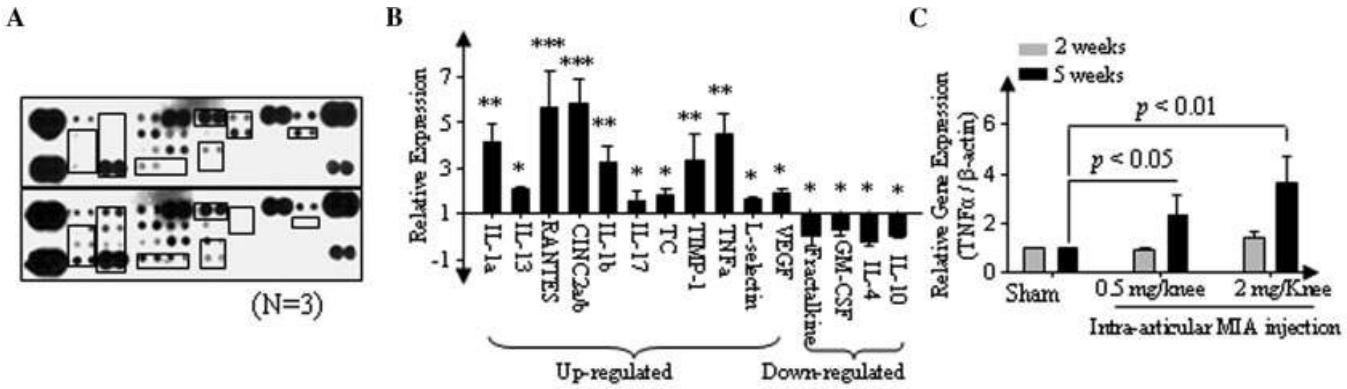

Figure 5. Cytokine profiling in the lumbar spinal cord in the MIA-induced rat OA model. Rats were administered a single intraarticular injection of MIA (2 mg per knee) or saline (sham) and were killed 2 weeks or 5 weeks after injection. Lumbar spinal cords were harvested. **A,** Antibody array membranes incubated with the spinal cord tissue lysates (week 5) from the sham-treated animals (upper panel) and the animals with MIA-induced knee joint pain (lower panel). **B,** Levels of selected cytokines in MIA-treated animals (relative to levels in sham-treated animals [set at 1]); only cytokines whose levels were altered in the experimental group are shown. Values are the mean and SEM. $* = P < 0.05$; $** = P < 0.01$; $*** = P < 0.001$, versus sham treatment. **C,** Relative expression of TNFα mRNA in the spinal dorsal horn, analyzed by real-time polymerase chain reaction. Values are the mean and SEM. CINC2a/b = cytokine-induced neutrophil chemoattractant 2α/β; TC = thymus chemokine; TIMP-1 = tissue inhibitor of metalloproteinases 1; VEGF = vascular endothelial growth factor; GM-CSF = granulocyte–macrophage colony-stimulating factor (see Figure 4 for other definitions).

gether, these findings indicate that neuropathic pain mechanisms may be fundamental to the etiology of OA pain, independent of the biologic factors that have been proposed to be involved in the symptoms of OA.

Spinal response to the MIA-induced knee OA pain model. Peripheral sensitization is characterized by the interplay between peripheral nociceptors and inflammation, and may initiate osteoarthritic joint pain via central sensitization (34,35). Because central sensitization involves enhanced excitability of neurons, we examined spinal responses provoked by MIA-induced chronic knee joint pain. Protein expression profiling was performed using a cytokine antibody array that permits simultaneous quantitative detection of anti- and proinflammatory cytokines. Spinal dorsal horn tissue protein extracts were prepared from carefully dissected ipsilateral dorsal horn of the lumbar spinal cord of rats administered saline or 2 mg MIA. Tissue lysates from the dorsal horn of the spinal cord were prepared after 5 weeks, and incubated with array membranes to monitor alterations in cytokine levels (Figure 5A).

Quantitative changes in cytokine protein levels were measured by densitometric analysis (Figure 5B). The results revealed significant increases in levels of multiple proinflammatory cytokines and chemokines (IL-1α and IL-1β, RANTES, cytokine-induced neutrophil chemoattractant 2α/β, IL-17, thymus chemokine, TNFα, L-selectin, and vascular endothelial growth factor [VEGF]). Unexpectedly, we observed a reduction in the expression of fractalkine, an acute spinal injury pain–associated chemokine (36), and granulocyte–macrophage colony-stimulating factor (both $P < 0.05$). We also found a robust reduction in antiinflammatory factors, i.e., IL-4 and IL-10 (both $P < 0.05$). However, the antiinflammatory factor IL-13 was increased at the spinal level in animals with OA-induced pain.

To assess whether cytokine protein levels correlate with corresponding changes in messenger RNA (mRNA) levels within the cellular components of the spinal cord (i.e., glia and neurons), we examined TNFα mRNA as a representative pain-associated cytokine that is highly up-regulated at the protein level in the spinal cord due to OA-induced knee joint pain. Real-time PCR demonstrated that the expression of TNFα was substantially increased in the late stages of OA-induced pain (week 5), but not during an earlier stage (week 2) (Figure 5C). These results suggest that modulation in the expression of TNFα, and perhaps other cytokines, contributes to the development of chronic pain in OA.

DISCUSSION

The present study provides new insights into molecular mechanisms by which nociceptive pathways are associated with chronic pain in OA. Our results confirm that the MIA-induced OA model in the rat is suitable for mechanistic and pharmacologic studies on symptomatic pain caused by OA. We correlated alter-

ations in the central compartments (DRGs and the spinal cord) with structural changes in components of the peripheral knee joint and symptomatic pain. Our findings provide key in vivo evidence that OA pain is caused by central sensitization of the nociceptive pathways. The data further suggest that nociceptive signals are transduced from the affected peripheral OA region to central compartments to overproduce inflammatory cytokines and pain mediators at the level of the sensory neurons and spinal cord.

Animal models have provided useful tools for investigating neuropathic or inflammatory pain (13). Generation of animal models for studying OA pain has been more challenging because it requires induction of gradual structural changes associated with the sustained chronic pain while avoiding severe inflammation or direct nerve damage.

The MIA-induced OA model was first described by Kalbhen (37) and is highly reproducible, with predictable pain behavior responses. The model demonstrates a clear interrelationship between structural knee joint components, including cartilage, synovium, and subchondral bone, and corresponding pain behavior. Histopathologic features of the knee joint after intraarticular injection of MIA have been found to mimic those seen in human OA (16–25,37,38). Our present data corroborate these previous reports. Furthermore, findings of our dose-response and time course studies suggest that the disease induced by intraarticular injection of 0.5 mg MIA per knee joint could be representative of early OA at 2 weeks postinjection, and of end-stage OA at >4 weeks postinjection, exhibiting structural changes similar to those observed in human OA. However, Barve et al (15) suggested that the MIA-induced knee joint pain model and human OA are substantially different in terms of gene expression patterns. It is not clear at this point whether the differences described by those authors result from differences between the 2 species, and therefore, caution must be exercised in translating the data obtained from analyses of MIA-induced knee joint OA pain.

Blood vessel formation is substantially increased in the synovium in knee joints of OA patients compared with normal human tissue (Collins grade 0 or 1). In the current study, MIA-induced OA knee joint pain was associated with increased neovascularization, as is found in late-stage human OA. The increase in angiogenesis in the animal model was significant at the week-5 time point; however, we did not observe prominent angiogenic features in rats at 2 weeks after MIA injection, suggesting that angiogenesis progresses slowly. It is possible that extensive angiogenesis, as is characteristic of advanced human OA, may not develop until 4–5 weeks after the administration of MIA in the animal model (end-stage OA). Slow progression of angiogenesis in our animal model may resemble findings in the early stages of human OA (Collins grade 2 or 3), in which significant increases in angiogenesis in knee joint synovium have not been detected (29). Synovial neovascularization is frequently accompanied by inflammation ("synovitis") in human OA (33) and largely driven by secretion of angiogenic factors (i.e., basic fibroblast growth factor, VEGF) and inflammatory cytokines, by lymphocytes that initiate a positive feedback loop (10,33). Thus, it is possible that angiogenesis may facilitate the sustained chronic pain in OA, as has been proposed previously (33).

Our comparison of several OA animal models including the MIA-injected knee OA model and neuropathic pain models reveals that OA pain pathways may overlap, at least in part, with neuropathic pain mechanisms. Our results suggest that OA-induced pain is associated with central sensitization, perhaps via neuronal and glial cellular activity. MIA-induced alterations of sensory neuronal responses to OA pain were also observed upon destabilization of the knee joint by ACLT, a well-established OA animal model. Our results are consistent with the previous observation that MIA-injected rats become responsive to medication that is normally prescribed for chronic and neuropathic pain (39–44).

Peripheral sensitization, which is the result of increased activity of peripheral nociceptors by inflammation, leads to central sensitization, which involves enhanced excitability of cellular components of spinal cord (i.e., glia and neurons) (44). Results of expression profiling using cytokine antibody arrays and real-time PCR analyses revealed that cellular components of the spinal cord respond to OA-induced pain by modulating levels of multiple cytokines. Some of the cytokines that were elevated in OA-induced pain are well-characterized pain mediators that promote central sensitization in other animal models of pain, such as neuropathic pain (42–44). We do not yet know which cytokines and what signaling components triggered by these cytokines are rate-limiting targets that control central sensitization caused by OA. Further studies using the MIA-induced OA pain model, which is a useful tool for investigation of the onset and progression of chronic nociceptive pain mechanisms, may ultimately lead to the development of a new class of molecular medicines that could effectively alleviate knee pain caused by degener-

ative joint diseases such as OA. Future studies with the objective of developing "OA-specific analgesic drugs" can build on the principal conclusion of the current study, i.e., that the dynamic interactions between peripheral knee joint tissue and central sensitization may occur through nociceptive pain pathways.

ACKNOWLEDGMENTS

We would like to thank the tissue donors, Dr. Arkady Margulis, and the Gift of Hope Organ and Tissue Donor Network for providing normal human joint tissue samples, and Dr. Gabriella Cs-Szabo and Orthopedic Tissue Repository Studies for providing OA tissue. We thank Dr. Carol Muehleman for her thoughtful discussions on microscopic observations and morphologic changes in structural knee joint components, and Dr. John Cavanaugh (Wayne State University, Detroit, MI) for generously sharing his expertise on sensory innervations and musculoskeletal pain. We also appreciate the support of the Department of Anesthesiology at Rush University Medical Center in allowing us access to the institutional animals and surgery facility. We express sincere gratitude to Dr. Jinyuan Li and Boris Jozic for their help during animal surgery and pain assessments.

AUTHOR CONTRIBUTIONS

All authors were involved in drafting the article or revising it critically for important intellectual content, and all authors approved the final version to be published. Dr. Im had full access to all of the data in the study and takes responsibility for the integrity of the data and the accuracy of the data analysis.

Study conception and design. Im, Kim, Li, van Wijnen, Desevré, Kroin.

Acquisition of data. Im, Kim, Li, Kotwal, Sumner, van Wijnen, Davis, Yan, Levine, Desevré, Kroin.

Analysis and interpretation of data. Im, Kim, Li, Sumner, van Wijnen, Henry, Desevré, Kroin.

REFERENCES

1. Sprangers MA, de Regt EB, Andries F, van Agt HM, Bijl RV, de Boer JB, et al. Which chronic conditions are associated with better or poorer quality of life? J Clin Epidemiol 2000;53:895–907.
2. Felson DT. The sources of pain in knee osteoarthritis. Curr Opin Rheumatol 2005;17:624–8.
3. Schuelert N, McDougall JJ. Electrophysiological evidence that the vasoactive intestinal peptide receptor antagonist VIP6-28 reduces nociception in an animal model of osteoarthritis. Osteoarthritis Cartilage 2006;14:1155–62.
4. Schaible HG, Grubb BD. Afferent and spinal mechanisms of joint pain. Pain 1993;55:5–54.
5. Just S, Pawlak M, Heppelmann B. Responses of fine primary afferent nerve fibres innervating the rat knee joint to defined torque. J Neurosci Methods 2000;103:157–62.
6. Broom N, Chen MH, Hardy A. A degeneration-based hypothesis for interpreting fibrillar changes in the osteoarthritic cartilage matrix. J Anat 2001;199:683–98.
7. Arlet J, Ficat P, Mazieres B. Coxarthroses due to ischemia: ischemic coxarthropathy. Rev Rhum Mal Osteoartic 1978;45: 549–60. In French.
8. Dye SF, Vaupel GL, Dye CC. Conscious neurosensory mapping of the internal structures of the human knee without intraarticular anesthesia. Am J Sports Med 1998;26:773–7.
9. Im HJ, Li X, Muddasani P, Kim GH, Davis F, Rangan J, et al. Basic fibroblast growth factor accelerates matrix degradation via a neuro-endocrine pathway in human adult articular chondrocytes. J Cell Physiol 2008;215:452–63.
10. Im HJ, Muddasani P, Natarajan V, Schmid TM, Block JA, Davis F, et al. Basic fibroblast growth factor stimulates matrix metalloproteinase-13 via the molecular cross-talk between the mitogen-activated protein kinases and protein kinase Cδ pathways in human adult articular chondrocytes. J Biol Chem 2007;282: 11110–21.
11. Li X, Ellman M, Muddasani P, Wang JH, Cs-Szabo G, van Wijnen AJ, et al. Prostaglandin E_2 and its cognate EP receptors control human adult articular cartilage homeostasis and are linked to the pathophysiology of osteoarthritis. Arthritis Rheum 2009;60: 513–23.
12. Muddasani P, Norman JC, Ellman M, van Wijnen AJ, Im HJ. Basic fibroblast growth factor activates the MAPK and NFκB pathways that converge on Elk-1 to control production of matrix metalloproteinase-13 by human adult articular chondrocytes. J Biol Chem 2007;282:31409–21.
13. Bendele A, McComb J, Gould T, McAbee T, Sennello G, Chlipala E, et al. Animal models of arthritis: relevance to human disease. Toxicol Pathol 1999;27:134–42.
14. Neugebauer V, Han JS, Adwanikar H, Fu Y, Ji G. Techniques for assessing knee joint pain in arthritis. Mol Pain 2007;3:8.
15. Barve RA, Minnerly JC, Weiss DJ, Meyer DM, Aguiar DJ, Sullivan PM, et al. Transcriptional profiling and pathway analysis of monosodium iodoacetate-induced experimental osteoarthritis in rats: relevance to human disease. Osteoarthritis Cartilage 2007;15:1190–8.
16. Bendele AM, Hulman JF. Spontaneous cartilage degeneration in guinea pigs. Arthritis Rheum 1988;31:561–5.
17. Gustafson SB, Trotter GW, Norrdin RW, Wrigley RH, Lamar C. Evaluation of intra-articularly administered sodium monoiodoacetate-induced chemical injury to articular cartilage of horses. Am J Vet Res 1992;53:1193–202.
18. Pond MJ, Nuki G. Experimentally-induced osteoarthritis in the dog. Ann Rheum Dis 1973;32:387–8.
19. Moskowitz RW, Davis W, Sammarco J, Martens M, Baker J, Mayor M, et al. Experimentally induced degenerative joint lesions following partial meniscectomy in the rabbit. Arthritis Rheum 1973;16:397–405.
20. Combe R, Bramwell S, Field MJ. The monosodium iodoacetate model of osteoarthritis: a model of chronic nociceptive pain in rats? Neurosci Lett 2004;370:236–40.
21. Guzman RE, Evans MG, Bove S, Morenko B, Kilgore K. Monoiodoacetate-induced histologic changes in subchondral bone and articular cartilage of rat femorotibial joints: an animal model of osteoarthritis. Toxicol Pathol 2003;31:619–24.
22. Piscaer TM, Waarsing JH, Kops N, Pavljasevic P, Verhaar JA, van Osch GJ, et al. In vivo imaging of cartilage degeneration using microCT-arthrography. Osteoarthritis Cartilage 2008;16:1011–7.
23. Clements KM, Ball AD, Jones HB, Brinckmann S, Read SJ, Murray F. Cellular and histopathological changes in the infrapatellar fat pad in the monoiodoacetate model of osteoarthritis pain. Osteoarthritis Cartilage 2009;17:805–12.
24. Kobayashi K, Imaizumi R, Sumichika H, Tanaka H, Goda M, Fukunari A, et al. Sodium iodoacetate-induced experimental osteoarthritis and associated pain model in rats. J Vet Med Sci 2003;65:1195–9.
25. Bove SE, Calcaterra SL, Brooker RM, Huber CM, Guzman RE, Juneau PL, et al. Weight bearing as a measure of disease progression and efficacy of anti-inflammatory compounds in a model of

monosodium iodoacetate-induced osteoarthritis. Osteoarthritis Cartilage 2003;11:821–30.
26. Glasson SS, Blanchet TJ, Morris EA. The surgical destabilization of the medial meniscus (DMM) model of osteoarthritis in the 129/SvEv mouse. Osteoarthrithis Cartilage 2007:15:1061–9.
27. Hargreaves K, Dubner R, Brown F, Flores C, Joris J. A new and sensitive method for measuring thermal nociception in cutaneous hyperalgesia. Pain 1988;32:77–88.
28. Chaplan SR, Bach FW, Pogrel JW, Chung JM, Yaksh TL. Quantitative assessment of tactile allodynia in the rat paw. J Neurosci Methods 1994;53:55–63.
29. Collins DH. The pathology of articular and spinal diseases. London: Edward Arnold; 1949.
30. Vincent TL, Saklatvala J. Is the response of cartilage to injury relevant to osteoarthritis? [editorial]. Arthritis Rheum 2008;58: 1207–10.
31. Appleton CT, McErlain DD, Pitelka V, Schwartz N, Bernier SM, Henry JL, et al. Forced mobilization accelerates pathogenesis: characterization of a preclinical surgical model of osteoarthritis. Arthritis Res Ther 2007;9:R13.
32. McDougall JJ, Watkins L, Li Z. Vasoactive intestinal peptide (VIP) is a modulator of joint pain in a rat model of osteoarthritis. Pain 2006;123:98–105.
33. Bonnet CS, Walsh DA. Osteoarthritis, angiogenesis and inflammation. Rheumatology (Oxford) 2005;44:7–16.
34. McDougall JJ. Arthritis and pain: neurogenic origin of joint pain. Arthritis Res Ther 2006;8:220.
35. Harvey VL, Dickenson AH. Behavioural and electrophysiological characterisation of experimentally induced osteoarthritis and neuropathy in C57Bl/6 mice. Mol Pain 2009;5:18.
36. Verge GM, Milligan ED, Maier SF, Watkins LR, Naeve GS, Foster AC. Fractalkine (CX3CL1) and fractalkine receptor (CX3CR1) distribution in spinal cord and dorsal root ganglia under basal and neuropathic pain conditions. Eur J Neurosci 2004;20:1150–60.
37. Kalbhen DA. Chemical model of osteoarthritis—a pharmacological evaluation. J Rheumatol 1987;14:130–1.
38. Janusz MJ, Hookfin EB, Heitmeyer SA, Woessner JF, Freemont AJ, Hoyland JA, et al. Moderation of iodoacetate-induced experimental osteoarthritis in rats by matrix metalloproteinase inhibitors. Osteoarthritis Cartilage 2001;9:751–60.
39. Vonsy JL, Ghandehari J, Dickenson AH. Differential analgesic effects of morphine and gabapentin on behavioural measures of pain and disability in a model of osteoarthritis pain in rats. Eur J Pain 2009;13:786–93.
40. Ivanavicius SP, Ball AD, Heapy CG, Westwood FR, Murray F, Read SJ. Structural pathology in a rodent model of osteoarthritis is associated with neuropathic pain: increased expression of ATF-3 and pharmacological characterisation. Pain 2007;128:272–82.
41. Fernihough J, Gentry C, Malcangio M, Fox A, Rediske J, Pellas T, et al. Pain related behaviour in two models of osteoarthritis in the rat knee. Pain 2004;112:83–93.
42. Cheng HY, Pitcher GM, Laviolette SR, Whishaw IQ, Tong KI, Kockeritz LK, et al. DREAM is a critical transcriptional repressor for pain modulation. Cell 2002;108:31–43.
43. Xiao HS, Huang QH, Zhang FX, Bao L, Lu YJ, Guo C, et al. Identification of gene expression profile of dorsal root ganglion in the rat peripheral axotomy model of neuropathic pain. Proc Natl Acad Sci U S A 2002;99:8360–5.
44. Gardell LR, Wang R, Ehrenfels C, Ossipov MH, Rossomando AJ, Miller S, et al. Multiple actions of systemic artemin in experimental neuropathy. Nat Med 2003;9:1383–9.

DOI 10.1002/art.27746

Errata

In several articles published in 2009–2010, the affiliation information for one of the authors/contributors, Dr. Paul Emery, was incomplete. Dr. Emery's affiliation should have been listed as University of Leeds and NIHR Leeds Musculoskeletal Biomedical Research Unit, Leeds, UK. The articles on which Dr. Emery was an author were as follows: Barkham et al, Arthritis Rheum April 2009 (pages 946–954), Bennett et al, Arthritis Rheum May 2009 (pages 1331–1341), Vital et al (letter), Arthritis Rheum June 2009 (page 1867), Saleem et al, Arthritis Rheum July 2009 (pages 1915–1922), Emery et al, Arthritis Rheum August 2009 (pages 2272–2283), Morgan et al, Arthritis Rheum September 2009 (pages 2565–2576), Emery et al, Arthritis Rheum March 2010 (pages 674–682), Jones et al, Arthritis Rheum July 2010 (pages 1944–1954), and Seibold et al, Arthritis Rheum July 2010 (pages 2101–2108). The article on which Dr. Emery was a contributor listed in the appendix was Ginzler et al, Arthritis Rheum January 2010 (pages 211–221).

We regret the errors.